DISTRIBUTED REPRESENTATIONS FOR ACTIN-MYOSIN INTERACTION IN THE OSCILLATORY CONTRACTION OF MUSCLE

JOHN THORSON *and* D. C. S. WHITE

From the A. R. C. Unit of Insect Physiology, Department of Zoology, Oxford University, Oxford, England. Dr. Thorson's present address is the Department of Neurosciences, School of Medicine, University of California at San Diego, LaJolla, California 92037.

ABSTRACT In this paper we suggest and test a specific hypothesis relating the attachment-detachment cycle of cross bridges between actin (I) and myosin (A) filaments to the measured length-tension dynamics of active insect fibrillar flight muscle. It is first shown that if local A-filament strain perturbs the rate constants in the cross-bridge cycle appropriately, then exponentially delayed tension changes can follow imposed changes of length; the latter phenomenon is sufficient for the work-producing property of fibrillar muscle, as measured with small-signal forcing of length and at low Ca^{2+} concentration, and possibly for related effects described recently in frog striated muscle. It is not clear a priori that the above explanation of work production by fibrillar muscle will remain tenable when the viscoelastic complexity of the heterogeneous sarcomere is taken into account. However, White's (1967) recent mechanical and electron microscope study of the passive dynamics of glycerinated fibrillar muscle has produced a model of the distributed viscoeleastic structure sufficiently explicit that alternative schemes for cross-bridge force generation in this muscle can now be tested more critically than previously. Therefore, we derive and solve third-order partial-differential equations which relate local interfilament shear forces associated with the perturbed cross-bridge cycles to the over-all length-tension dynamics of an idealized sarcomere. We then show (*a*) that the starting hypothesis can account approximately for the small-signal dynamics of glycerinated muscle in the work-producing state over two decades of frequency and (*b*) that the rate constants for cross-bridge formation and breakage, restricted solely by fitting of the model to the mechanical data, determine a cycling rate of cross bridges in the model compatible with recent measurements of ATP hydrolysis rate vs. stretch in this muscle. Finally, the formulation is extended tentatively to the large-signal nonlinear case, and shown to compare favorably with previous suggestions for the origin of the work-producing dynamics of fibrillar flight muscle.

INTRODUCTION

Contraction of a striated muscle fiber involves an interaction between the actin (I) and the myosin (A) filaments, but the nature of this interaction is at present un-

known. In this paper a number of simple hypotheses about the events occurring in the interaction are considered. The general approach is related to that of A. F. Huxley (1957) in that it is based on a cycle of activity of the cross bridge on the myosin filament. Methods are developed which allow consequences of these hypotheses to be compared with the behavior of muscle preparations for which small-signal length-tension dynamics have been measured. Such preparations now include glycerinated insect flight muscle (Jewell and Rüegg, 1966; Abbott, 1968[1]) and frog semitendinosus muscle (Armstrong et al., 1966).

The special mechanical properties of insect asynchronous flight muscle were first described by Pringle (1949) who observed that in the blow fly the frequency of muscle action potentials (about 3/sec) did not correspond to the frequency of contraction of the flight muscles (about 120/sec). This result implied that the events producing the contractile force in the muscle could be brought into temporal synchrony by some factor other than the arrival of a nerve impulse; hence the term "asychronous." Subsequent work (reviewed by Pringle 1957, 1967) has confirmed this view, and has made clear that externally induced changes of muscle length (whether due to inertia of a natural load or artificially imposed) cause this muscle to respond with delayed changes in tension. The phenomenon of activation of the muscle by induced length changes will be termed "stretch activation," to distinguish it from the more familiar form of activation by means of an action potential. Recent work on glycerinated muscle (Jewell and Rüegg, 1966; Abbott and Chaplain, 1966) suggests that the mechanism of stretch activation in insect muscle resides in the myofibrillar structure itself.

Cross bridges, which are attached to the myosin filaments (H. E. Huxley, 1957) have often been implicated as the site of the interaction between the A and I filaments (A. F. Huxley, 1957; H. E. Huxley, 1964). Pringle (1965)[2] has pointed out that effective interaction between different cross bridges may occur if their activity is dependent upon stress in one or other of the filaments; local A-I filament interaction may produce strain in other parts of the filaments which can in turn affect the activity of the bridges at these positions. Thus, in order to compare hypothetical time-dependent events at the macromolecular level with length-tension dynamics of a whole sarcomere or myofibril, one must take account of the distributed viscoelastic properties of the filament array. The results of White's (1967, 1968[3]; see also Pringle, 1967) study of the passive dynamics of insect flight muscle make it possible to calculate consequences of such effects in a quantitative manner.

In this paper it is first shown that the dynamics of cross-bridge detachment and attachment, if perturbed by a factor which is directly linked to length changes in the sarcomere, provide a possible explanation for the delay in tension following induced

---

[1] Abbott, R. H. 1968. Paper in preparation.
[2] Pringle, J. W. S. 1965. Personal communication.
[3] White, D. C. S. 1968. Paper in preparation.

length changes. Then, in order to see whether this hypothesis remains tenable when the distributed viscoelastic properties of the muscle are taken into account, a set of partial differential equations for an idealized viscoelastic sarcomere is derived in which the dynamic cross-bridge cycle determines the local shear force generated between the actin and myosin filaments. The active length-tension dynamics associated with this hypothetical structure are then compared quantitatively with both mechanical and biochemical experiments. The consequences of certain variations in the assumptions and parameters are also considered, to the extent that the methods permit.

EXPERIMENTAL BACKGROUND

Apart from the well-documented demonstration that insect asynchronous muscle can perform oscillatory work (that is, that imposed sinusoidal length changes induce delayed sinusoidal tension changes) in a nearly linear fashion (Boettiger, 1957; Pringle, 1957; Machin and Pringle, 1960), there are several more recent results which are critical to the arguments to be developed in this paper.

(*a*) Glycerinated flight muscle from the genus *Lethocerus* (a tropical giant water bug) was shown by Jewell and Rüegg (1966) to perform oscillatory work if Ca^{2+} and ATP are provided. R. H. Abbott and Chaplain (1966) further showed that treatment with the nonionic detergent "Tween 80" did not eliminate this capacity, even though membrane systems and mitochondria were apparently largely destroyed or removed. It was suggested, therefore, that the mechanism of delayed tension following stretch resides in the myofibrillar structure itself.

(*b*) Rüegg and Tregear (1966) and Chaplain (1967) have demonstrated that at low degrees of stretch the rate of hydrolysis of ATP increases with the degree of steady stretch. Calcium is apparently required for stretch activation to occur. The view that such stretch activation is a central specialization of asychronous muscle is further suggested from the form of the relationship between the rate of hydrolysis of ATP and the Ca^{2+} concentration. It has been shown that, for actomyosin gels and myofibril suspensions, the ATPase activity of insect asynchronous muscle is activated to a smaller extent by Ca^{2+} than that of rabbit muscle or insect synchronous leg muscle (vom Brocke, 1966; Maruyama, Pringle, and Tregear, 1968).

(*c*) Reedy, Holmes, and Tregear (1965), using both electron microscopy and X-ray diffraction, showed that many of the cross bridges in relaxed flight muscle appeared perpendicular to the myosin and detached from the actin filaments. In the rigor state, however, the preferred arrangement of bridges was attached and angled to the filament array at about 45°. Combined with biochemical evidence (Mihalyi and Szent-Györgyi, 1953) associating the heavy-meromyosin portion of the myosin molecule with the enzyme activity of actomyosin, and with the suggestion that the heavy meromyosin constitutes the cross bridge (H. E. Huxley, 1963), the structural data add considerable weight to the general notion that muscle force is due to attached bridges between actin and myosin filaments, seeking a position of minimum configurational potential energy.

(*d*) Abbott[1] has discovered that, at very low concentrations of Ca^{2+}, glycerinated water-bug flight muscle performs typical oscillatory work at low frequencies, but that at high frequencies the active and passive frequency-response curves become nearly indistinguishable. With higher concentrations of Ca^{2+} the entire activated frequency-response curve shifts as though a parallel elastic component had been reduced—giving dynamic length-tension curves similar to those previously reported at high Ca^{2+} concentration (Machin and Pringle, 1960; Abbott and Chaplain, 1966). As Abbott[1] points out, this finding suggests that calcium has a dual role in its

influence on the mechanical response of the muscle. For example, the low-Ca^{2+} data may represent the requirement for Ca^{2+} of a stretch-activation mechanism which has rather simple low-pass-filter kinetics, whereas higher Ca^{2+} concentration may change, among other things, the elastic properties of the filaments. The low-Ca^{2+} oscillatory work therefore represents the dynamics of the active process in the simpler form, and in this paper we compare our small-signal formulation with Abbott's data for the low-Ca^{2+} state.

(*e*) White (1967, 1968[3]) has measured the dynamics of water-bug glycerinated muscle in the relaxed and rigor states, and has derived values for the viscous and elastic properties of the known structure. Results of that analysis are used to specify the passive parameters of the active muscle treated in this paper.

(*f*) Electron microscope studies (Auber and Couteaux, 1963) have suggested that in dipteran flight muscle, an asynchronous muscle, "C (connecting) filaments" (terminology of White, 1967) connect the Z-line material to the ends of the A filaments. Although such filaments have not been observed in all asynchronous muscle (Ashhurst, 1967), the existence of some means of placing very-low-frequency or maintained stress on the A filaments is consistent with the high passive stiffness of these muscles, and also with the stretch-activation properties.

In a separate paper (White, 1968[3]) the mathematical methods developed in this paper are used to study the mechanical properties of the sarcomere in the relaxed state, and alternative representations of the C-filament region are discussed.

REPRESENTATION OF LOCAL CROSS-BRIDGE ACTIVITY

In this section a model for local generation of cross-bridge force is specified. The word "local" is used to denote "at a given distance along the sarcomere from the Z-line." It will be shown that a simple dynamic balance of attached and detached cross bridges is especially appropriate to the small-displacement experiments under consideration, and that this representation leads naturally to a specific hypothesis for the origin of the delayed tension following stretch.

Past descriptions of the unidirectional force generation implicit in the contractile actin-myosin interaction include:

(*a*) a spatial distribution of attachment rate for actin-myosin links which is biased towards one side of their preferred minimum-potential-energy position, as in the example worked by A. F. Huxley (1957). Davie's (1963) view of "contracting" bridges involves a related bias.

(*b*) an asymmetrically located actin-attachment site on the heavy-meromyosin "bridge" (Perry, 1965).

(*c*) a net bias of force as the result of a "vernier effect" (Spencer and Worthington, 1960) or net attraction (Ingels and Thompson, 1966) among attractive sites having different periodicities along the actin and myosin filaments.

In addition to the requirement for a directional force, a notion which is implicit in the consideration of a bridge's contribution to shear force between A and I filaments is that of a cycle of bridge activity. Only A. F. Huxley (1957), to our knowledge, has formulated and worked out quantitatively the consequences of a specific version of such a cycle. He confined his predictions to the constant-velocity dynamics of verte-

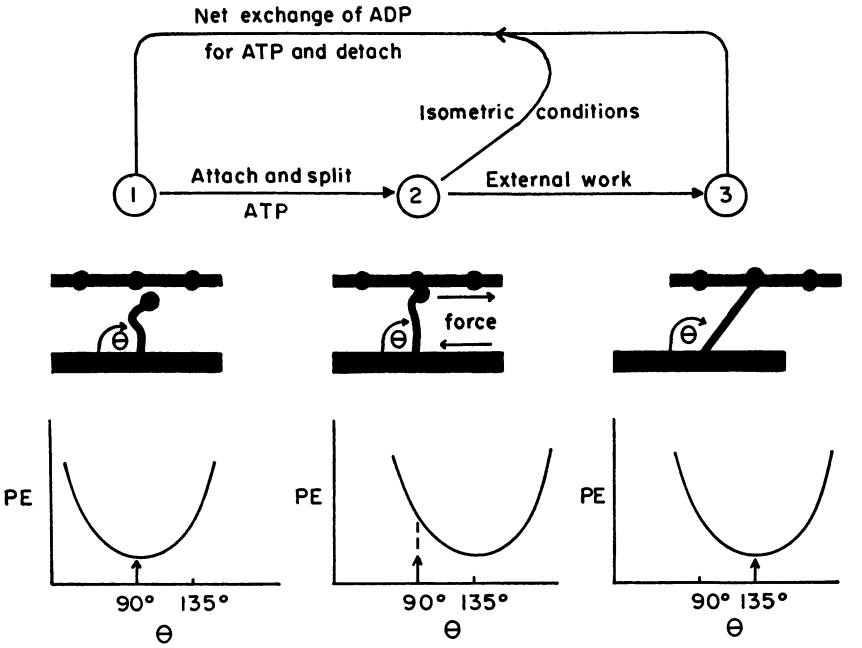

FIGURE 1 One visualization of the mechanical states involved as a cross bridge between actin and myosin filaments contributes cyclically to the interfilament shear force. The dots on the actin are not monomers, but are for visual reference. PE denotes the configurational potential energy of the local actin-bridge-myosin system. The labeled mechanical states denote (1) detachment, (2) attachment with local movement yielding negligible change in the slope of the PE vs. angle relationship, and (3) attachment in which the above slope does change appreciably.

brate striated muscle, but discussed the relation of the cycle to the shortening-relaxation implicit in insect-fibrillar-muscle behavior.

Consider a variant of the two-state (attached-detached) cycle presented by A. F. Huxley. Fig. 1 illustrates one general view of these states (the diagram conforms to the structural findings of Reedy, Holmes, and Tregear (1965) but the treatment is not restricted to this structural interpretation). The net result of attachment and splitting of a small number of molecules of ATP by a bridge, on this view, is that the curve relating the configurational potential energy of the local myosin-bridge-actin system to position is displaced, or changed in shape, so that the indicated shear force arises. As in Huxley's example, there is then a certain probability per unit time (or detachment rate constant) that the system will return to state 1.

Note that the cyclic behavior of the system of Fig. 1 is very much influenced both by the potential-energy shape and by any variation of detachment probability as the filaments slide from state 2 to state 3. These rules are unknown and difficult to estimate. For example, if the deformation were Hookean the force would be propor-

tional to displacement from equilibrium; if it were purely electrostatic the force could be *inversely* proportional to displacement squared.

However, in ideal isometric experiments, or in small-signal fibrillar-muscle experiments (in which oscillatory work is readily measured at cyclic length changes of 0.05 %, corresponding to half-sarcomere length changes of a few angstroms), relative filament motion can be sufficiently small that variations in detachment rate and bridge force associated with displacement may be negligible; the small-signal behavior of the muscle may therefore be nearly independent of the way in which these factors depend upon displacement. For this reason it seems justified, in the first instance, to test a version of this cycle in which the attached-state force of a single bridge, and the net detachment rate constant, are both constant during the period of attachment. This simplified cycle then involves only states 1 and 2 in Fig. 1, and the fluctuations in local A-I filament shear force arise only because of changes in the local fraction of bridges in state 2 (attached).

In Fig. 2, the heavy lines illustrate this idealized cycle of cross-bridge activity. The independent variables x and t denote position along the sarcomere and time, respectively. $n(x, t)$ denotes the fraction of the local population of bridges which are in the attached state. This population may be thought of as all of the bridges in a thin transverse section of a fibril located at distance x from the Z-line. The local A-I shear force per unit length, $f(x, t)$ (proportional to $n(x, t)$), and external length control $L(t)$ interact via the viscoelastic properties of the filaments to determine local instantaneous A-filament strain $\sigma(x, t)$. For the sake of definiteness in the initial calculations it is assumed that local attachment rate $p_a(x, t)$ is proportional to local A-filament strain $\sigma(x, t)$ and that detachment rate $p_d(x, t)$ is constant in both x and t. This effect of strain upon attachment rate will be termed *strain activation.* Later, effects of some variations on these assumptions are calculated. The "chemical control" in Fig. 2 represents the fact that increasing Ca^{2+} concentration increases the slopes of both the ATPase rate and the tension vs. stretch relationship of the muscle. Therefore an activation coefficient Q (with units sec^{-1}) is defined by

$$p_a(x, t) = Q\sigma(x, t).$$

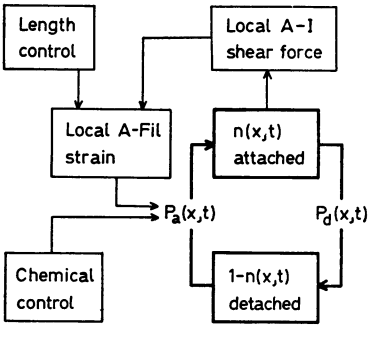

FIGURE 2 The tentative simplification of the cycle of Fig. 1, as discussed in the text, for the small-signal case.

For the cycle of Fig. 2,

$$\frac{\partial n(x, t)}{\partial t} = (1 - n(x, t))p_a(x, t) - n(x, t)p_d(x, t) \quad (1)$$

which is formally A. F. Huxley's (1957) first equation on page 286. For low Ca^{2+} concentrations and small amounts of steady stretch, it is assumed that the low tensions and stiffness increments observed imply that $n(x, t) \ll 1$ (equivalently, $p_a(x, t) \ll p_d(x, t)$)—i.e., only a small fraction of the bridges is in the attached state at any one time. Equation 1 can therefore be rewritten

$$\frac{\partial n(x, t)}{\partial t} = p_a(x, t) - n(x, t)p_d(x, t). \quad (1a)$$

Taking Laplace transforms of the terms of equation 1a under the above assumptions, and setting initial conditions to zero since only the transfer function relating $p_a(x, s)$ and $n(x, s)$ is required, one finds (in the Laplace variable s)

$$n(x, s) = \frac{Q}{s + p_d} \sigma(x, s).$$

A parameter F is now defined as the absolute maximum shear force per unit length produced by all available cross bridges (i.e., $f(x, t) = F$ when $n(x, t) = 1$), so that

$$f(x, s) = \frac{QF}{s + p_d} \sigma(x, s). \quad (2)$$

ORIGIN OF THE DELAYED TENSION FOLLOWING STRETCH

Equation 2 can be interpreted physically as follows: If imposed length changes were to induce nearly simultaneous A-filament strain throughout the sarcomere, and if total tension followed active A-I filament shear force rather closely, then the dynamic length-tension relation would be similar to the dynamic relation between $\sigma(x, s)$ and $f(x, s)$ in equation 2. This relation is simply that of a first-order low-pass filter (frequently called an exponential delay) with rate constant p_d. Since dynamics of this kind are similar to those measured between length and tension in the region of oscillatory work (Pringle, 1967; Abbott, 1968[1]), a natural hypothesis for the relevant delay is the physical basis of equation 2. On this view, therefore, the delay arises because it takes time to change the fraction of cross bridges attached, and the determining rate constant is the cross-bridge detachment rate p_d.

However, several factors may act to obscure the above effect. First, because of the distributed viscoelastic properties of the inhomogeneous sarcomere, average strain and shear force in the overlap region need not be strictly in phase with muscle length and tension, respectively. (A further complication, shown in Fig. 2, is that local shear force and local A-filament strain may reinforce one another.) Second, the detach-

ment rate constant may be sufficiently large that it is not rate limiting, in which case another process would determine the delay in question. The first of these difficulties is treated in the next section with a distributed viscoelastic representation of the entire sarcomere, in which equation 2 is used to represent a continuum of tension transfer between elastic A and I filaments. The second difficulty suggests that it may be instructive to compare cross-bridge cycling rate in the model (assuming that p_d is in fact rate limiting) with experimentally determined ATPase activity of the muscle.

THE RELATION OF CROSS-BRIDGE DYNAMICS TO THE LENGTH-TENSION DYNAMICS OF A HALF-SARCOMERE

Fig. 3 is an idealization of a half-sarcomere of insect fibrillar muscle. The filaments are represented as Hookean springs, and it is assumed that there is distributed viscous interaction both between the A and I filaments and between the C and I filaments. The assumptions underlying this representation, for the small-signal case, are made explicit in the Appendix. The relation of the model of Fig. 3 to the passive dynamics of fibrillar muscle is discussed more fully by White (1967, 1968[3]); although the treatment can be made more general by the inclusion of internal viscosity in the filaments, White has shown that the main frequency-dependent properties of the passive muscle, over several decades of frequency, can be described plausibly by the structure shown.

Here it is proposed to introduce the force due to attached cross bridges as a continuum of shear force between A and I filaments in the overlap region, and to calculate the resulting dynamic length-tension behavior of the sarcomere. The circled f in Fig. 3, therefore represents $f(x, s)$ in equation 2 with its specified dependence on local A-filament strain. The procedure, given in detail in the Appendix, is as follows: partial differential equations, in space and time, relating the (small) longitudinal displacements of points on the A and I filaments to the tensions in the system of Fig. 3 are derived for each region. Together with suitable boundary conditions, the equations establish a boundary-value problem which is solved analytically for the transfer function relating $L(s)$, the transform of the forced half-sarcomere length, to $T(s)$, the transform of the total tension in the system. Equation 22 in the Appendix is the resulting length-tension transfer function.

Characteristic rate constants for regions 1 and 2 of Fig. 3, for the passive muscle, are derived in the Appendix from inspection of the arguments of the exponential functions of equation 22. These rate constants are indicative of the frequency ranges in which passive stiffness changes most rapidly, and serve to guide analysis of the effects of the parameters. Furthermore, the effects of strain activation in equation 22 are attenuated at and above frequencies commensurate with bridge detachment rate p_d since $\eta(s)$, defined in equation 19, has in its denominator the factor $(s + p_d)$. The interactions of these effects are compared quantitatively with the experimental data in the next section, by assigning the value $j\omega$ (where $j = \sqrt{-1}$ and ω = angular fre-

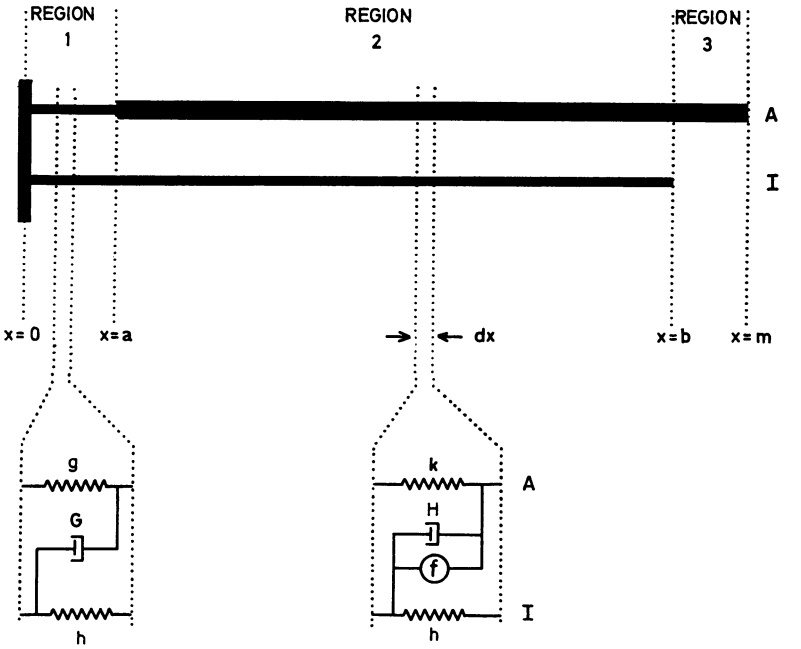

FIGURE 3 A half-sarcomere of insect fibrillar muscle, idealized mechanically for representation of small-displacement distributed viscoelastic behavior. Local cross-bridge shear force per unit length ($f(x, t)$ is indicated by the circled f. Partial differential equations for the three regions are derived in the Appendix, and the boundary-value problem is solved for length-tension dynamics of the sarcomere.

TABLE I

VALUES OF THE PARAMETERS USED TO DEFINE THE SARCOMERE IN FIG. 3

Parameter	Definition	Value	Units
k	A-filament stiffness times unit length	1.5×10^{-3}	dynes
g	C-filament stiffness times unit length	1.8×10^{-5}	dynes
h	I-filament stiffness times unit length	2.0×10^{-3}	dynes
H	A-I filament viscous interaction per unit length	3.2×10^{-6}	dyne-sec/micron^2
G	C-I filament viscous interaction per unit length	20	dyne-sec/micron^2
m	Half-sarcomere length	1.2	micron
a	C-filament length	0.05	micron
b	I-filament length per half-sarcomere	1.1	micron

quency) to s, and computing the length-tension frequency response. In tests of hypotheses about the cross-bridge dynamics, values of the passive-muscle parameters of Fig. 3 have been used which are consistent with the mechanical and electron microscopic analyses of White (1967, 1968[3]). These are given in Table I.

COMPARISON WITH EXPERIMENT

General Consequences of the Assumptions

Equation 22, derived in the Appendix, is simply a linear transfer function relating length and tension. Therefore the low-frequency or static effect of increasing the activation coefficient Q in the model (the correlate of Ca^{2+} concentration) is as in Fig. 4 *a*—stiffness is increased because strain induces cross-bridge attachment. This effect is not implausible as a first approximation—both tension and dynamic stiffness of the glycerinated water-bug muscle are increased when small amounts of Ca^{2+} are added to relaxing solution (Abbott[1]). In practice, there is also some increase of tension if a muscle at rest length ($L = 0$ in Fig. 4 *a*) is provided with Ca^{2+}. Although this property can be represented by introduction of a second strain-independent activation coefficient in equation 2, the linear length-tension dynamics are unaffected; the upper curve in Fig. 4 *a* is simply elevated without change in slope.

The hand-drawn curves of Fig. 4 *b* introduce schematically the dynamic behavior of equation 22, as determined by computation. As suggested by White's (1967) analysis of the passive dynamics, it has been assumed that the gradual low-frequency increase of stiffness is associated with the C-filament region, and that the high-frequency stiffness increase is due to the viscous interaction between A and I filaments. The solid curves in Fig. 4 *b* illustrate schematically the resulting dynamic behavior of the passive model (equation 22 with $Q = 0$), which agrees approximately with the experimental measurements of White (1967, 1968[3]). When Q, the activation coefficient, is increased, the effect shown by the dashed lines in Fig. 4 *b* is obtained.

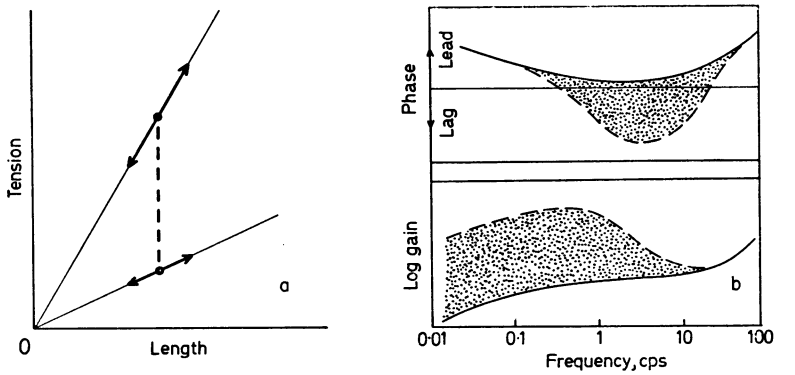

FIGURE 4 Qualitative properties of the linear formulation of equation 22. (*a*) Under static conditions, or at very low frequency, small-signal stiffness and total tension are increased in proportion (dotted lines) when the strain-activation coefficient Q is increased. (*b*) A schematic Bode diagram of the dynamic behavior of equation 22, discussed in the text. Solid lines: relaxed muscle. Dashed lines: activated. The phase diagram shows the phase difference between tension and length, and the gain diagram shows the logarithm of relative tension amplitude under constant-amplitude sinusoidal length perturbation, as a function of frequency.

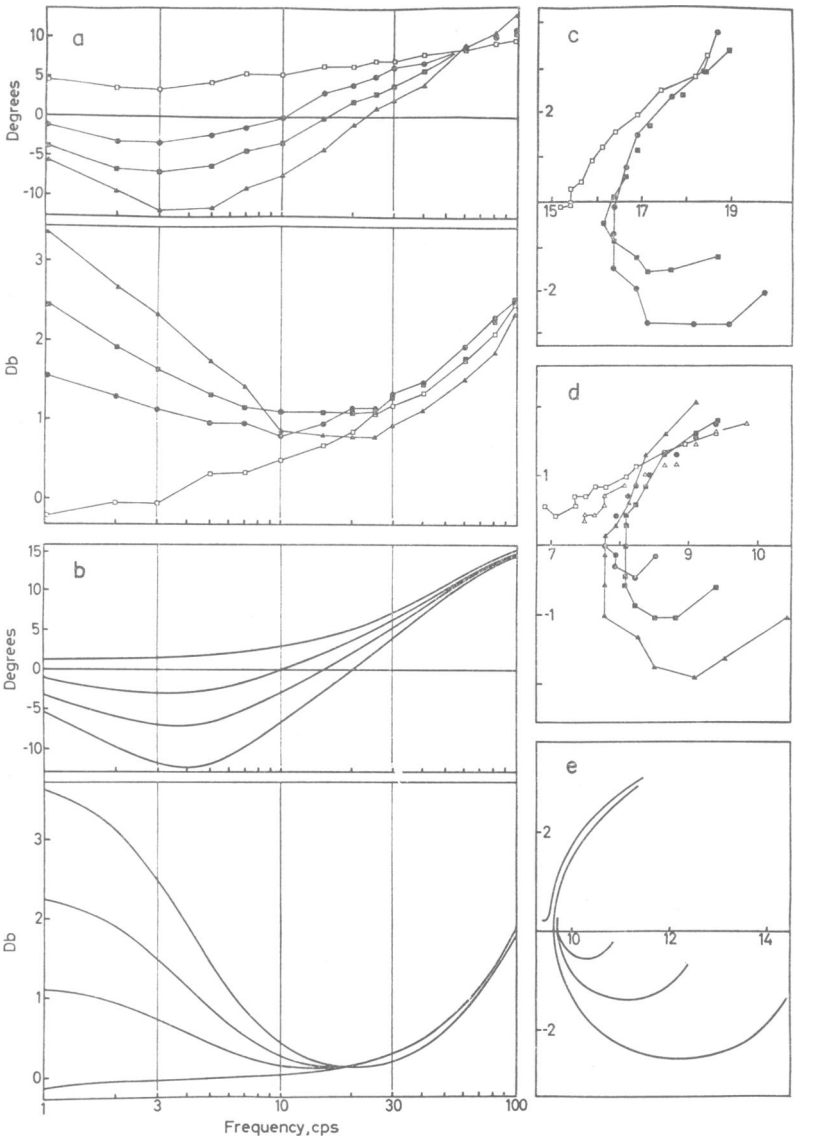

FIGURE 5 Comparison of experimental frequency-response data and the predicted response of the sarcomere of Fig. 3 as given by equation 22. (*a*) Bode plot of amplitude and phase of the tension response of glycerinated flight muscle of *Lethocerus cordofanus* against frequency, with respect to a constant-amplitude modulation of length (Abbott[1]). The preparation of the glycerinated muscle, and the chemical and mechanical conditions are as given by Abbott and Chaplain (1966). The experiments were done at the temperature 20°C. The response of the muscle is shown at a number of different Ca^{2+} concentrations. □: relaxed, pCa 8.5; ●: pCa 7.75; ■:pca 7.6; ▲:pCa 7.48. The convention used in the gain plot is that gain (in dB) = $20 \log_{10}$ (tension amplitude/constant reference level). (*b*) Bode plot of the frequency response computed from equation 22, plotted in a form identical to that of *a*. p_d has the value

Qualitatively, this is what would be expected if the low-pass filter property of equation 2 were mechanically in parallel with the passive structure of the muscle: at low frequency, the increased stiffness due to strain activation of cross-bridge force is in phase with length changes; the low-frequency gain increase and phase lead due to the stiffening of the C-filament region are still evident. At frequencies commensurate with the detachment rate, however, $n(x, t)$ can no longer follow $p_a(x, t)$ so that dynamic stiffness falls towards that of the passive muscle, with the expected phase lag in the region of this transition. As frequency is further increased, the phase lead and gain increase of the passive muscle dominate. Qualitatively, therefore, the suggestion that the delayed tension following stretch is due to the time required to change the fraction of bridges attached holds up well even when the viscoelastic complexity of Fig. 3 is taken into account. A more quantitative comparison with experiment is given in the next section.

The basis of oscillatory work, on this view, is as follows: associated with a given degree of steady stretch and Ca^{2+} concentration there is a particular cycling rate of bridges and a particular average fraction of bridges attached in each part of the sarcomere. When small length perturbations about this steady degree of stretch are imposed, exponentially delayed variations of $n(x, t)$, and hence of tension change, arise. Since $n(x, t) \ll 1$, the instantaneous cycling rate of bridges is about proportional to $p_a(x, t)$; and since the average value of $p_a(x, t)$ is constant, the small-signal cyclic work is done at no extra expenditure of chemical energy — the "maintenance heat" is simply reduced slightly as a consequence of advantageous redistribution of the "ATPase rate" over the cycle of oscillation. The possible origin of "extra ATPase on oscillation" (Rüegg and Tregear, 1966) measurable at relatively large amplitudes of oscillation, will be discussed later.

Small-Signal Length-Tension Dyanmics at Low Ca^{2+} Concentration

Fig. 5 *a* is a Bode plot of experimental length-tension frequency-response data (Abbott[1]) from glycerinated water-bug flight muscle at EGTA (ethylene glycol bis-(β-aminoethyl ether)-N,N′-tetraacetic acid) buffered Ca^{2+} concentrations in the range pCa = 8.3–7.5. Fig. 5 *b* shows the comparable response of tension in equation 22 to sinusoidal length forcing with appropriate values of the parameters. In obtain-

22.5 sec^{-1}, and the product ($Q \cdot F$) (in order of increasing low-frequency gain, and increasing phase-lag) set at 0.0, 0.011, 0.022, 0.037 dyne/micron-sec. The other parameters have the values given in Table I. (*c*) Nyquist plot as in *d*, but of a separate experiment, using *Lethocerus annulipes*, with the following values of pCa; □: (relaxed) 8.5; ■:8.28; ●:7.95. Temperature 20°C. (*d*) The experimental data of *a*, plotted in Nyquist-plot form. In this graph the abscissa represents the component of tension amplitude in-phase with length, and the ordinate the component of tension amplitude leading length by 90°. Both axes have the units dynes per fiber per per cent variation in length. The △ are from a repeat of the relaxed condition at the end of the experiment. (*e*) The frequency response predicted from equation 22 plotted in Nyquist-plot form. The parameter values are those used in *b*, and the units those of *d*.

ing this degree of agreement between equation 22 and the active data of Fig. 5 *a*, two parameters had been adjusted freely. These are the product $(Q \cdot F)$, which is effectively a single parameter (see below), and the detachment rate constant p_d (these have their effect in equation 22 through η); all other parameters are as restricted by White (1967) for the passive dynamics and given in Table I. It is an important point that the dynamic data restrict these two parameters separately, so that one cannot achieve an equivalent fit by changing one and adjusting the other. This restriction arises as follows: it is discernible from the form equation 22 in the Appendix, and confirmed by calculation, that the dynamic effects of activation are attenuated near a "corner frequency" nearly equal to $p_d/2\pi$, as would occur if p_d were the rate constant in a simple low-pass filter (see e.g., Brown, 1961). Thus with p_d near 22.5 sec^{-1}, as in Fig. 5 *b*, the experimental loss of activated stiffness and maximum phase lags near 3.5 cps, at 20°C, are simulated. Once p_d is fixed, and the elastic and dimensional parameters restricted to the values given in Table I, then the magnitude of the low-frequency or static stiffness increment on activation is determined by choice of the product $(Q \cdot F)$. The latter point is discernible in the form of equation 23 in the Appendix and from the four curves of Fig. 5 *b*, where $(Q \cdot F)$ is assigned the value zero and three nonzero values. Each value of $(Q \cdot F)$ can therefore be associated with the Ca^{2+} concentration pertaining to the corresponding experimental curve in Fig. 5 *a*.

Finally, it should be clear that Q and F appear in equation 22 only in the product $(Q \cdot F)$, reflecting the property of the low-Ca^{2+} model that if realizable bridge force per unit length, F, were increased, a smaller activation coefficient, Q, would compensate precisely. This ambiguity is removed below, where independent mechanical experiments are used to restrict F and to relate the resulting restriction on Q to biochemical activity in the muscle.

Figs. 5 *d* and 5 *e* reproduce the comparison of 5 *a* and 5 *b*, respectively, in the Nyquist-plot form. Fig. 5 *c* is a Nyquist plot of an independent experiment (Abbott[1]), illustrating the degree of reproducibility of the low-Ca^{2+} dynamics.

The main quantitative discrepancy between prediction and data can be seen to be associated with the shape of the *passive* dynamics, since the high-frequency stiffness increase vs. frequency is more gradual in the data than in the prediction. This situation is treated in more detail elsewhere (White[3]). In general the distributed viscoelastic system of Fig. 3 shows sharper stiffness transitions with frequency than does the muscle, so that one is led to consider that the parameters (such as k, h, and H) are not single-valued but rather are better represented in the muscle fiber by probability-distribution functions. Although this view is plausible, the relevant distributions are so difficult to restrict that we consider the approach of little assistance in the search for discrepancy between theory and experiment in this kind of system.

The above difficulty, and the experimental variability shown in Fig. 5, permit the conclusion that the active formulation is adequate for these data.

Sensitivity of the Predictions to Assumptions and Parameters

The agreement of Fig. 5 was obtained under the assumption that the attachment rate p_a is proportional to local strain in the A filaments. This type of activation was termed strain activation. An alternative assumption which also leads to a linear solution of the boundary-value problem is that local A-I filament displacement $(y(x, t) - z(x, t))$, rather than A-filament strain $(\partial y(x, t)/\partial x)$, perturbs $p_a(x, t)$.

Equation 2 then becomes

$$f(x, s) = \frac{RF}{s + p_d} \cdot (y(x, s) - z(x, s)) \qquad (2a)$$

where R is a new activation coefficient with units $\text{sec}^{-1}\text{cm}^{-1}$. This form of activation will be termed *displacement activation*. Although the frequency response of the system with displacement activation is distinct from that with strain activation (see below and Fig. 6), an appropriate choice of p_d leads to similar dynamic behavior in the region of the data of Fig. 5. The tests, therefore, do not restrict the particular parameter of mechanical deformation chosen to describe stretch activation, at least for the passive structure considered here.

Before more restrictive tests are described, it should be demonstrated that the distributed viscoelastic representation does interact with the active cycle of bridge force. The boundary-value problem established in the Appendix can be solved for a variety of effects relatable to experiment. These include the average distribution of strain over the sarcomere (which is a complicated exponential function of x) and the dynamic phase differences that occur in different parts of the overlap region. Here only one example will be presented—that of the effects of altering the A-filament stiffness k under both strain (Q) and displacement (R) activation. This prediction is of interest both with regard to Abbott's[1] suggestion that high Ca^{2+} concentration reduces the stiffness of the fibers, and with regard to White's (1967) demonstration that increasing the ionic strength of the relaxing solution produces large reversible changes in muscle stiffness. Fig. 6 shows the behavior of the length-tension transfer function (activated by Q in Fig. 6 *a*, and by R in Fig. 6 *b*) as k is reduced from the value determined by White (1967). p_d and all other parameters have been left identical in the two cases so that the loss of activated stiffness occurs at somewhat different frequencies. (For example, note the relative positions of the 10-cps points in Fig. 6 *a* IV and 6 *b* IV.) The interaction of the passive properties with the mode of activation is, however, clear: At very low frequencies the C region (defined in Fig. 3) becomes compliant so that A-filament strain, rather than A-I displacement, is the more attenuated. Hence the relatively greater reduction of low-frequency stiffness under strain activation in Fig. 6 *a* at large values of k (compare curves 6 *a* IV and 6 *b* IV). Moreover, as A-filament stiffness is reduced the A-filament strain for a given length change is increased; the relative loop sizes in Fig. 6 *a* for Q activation

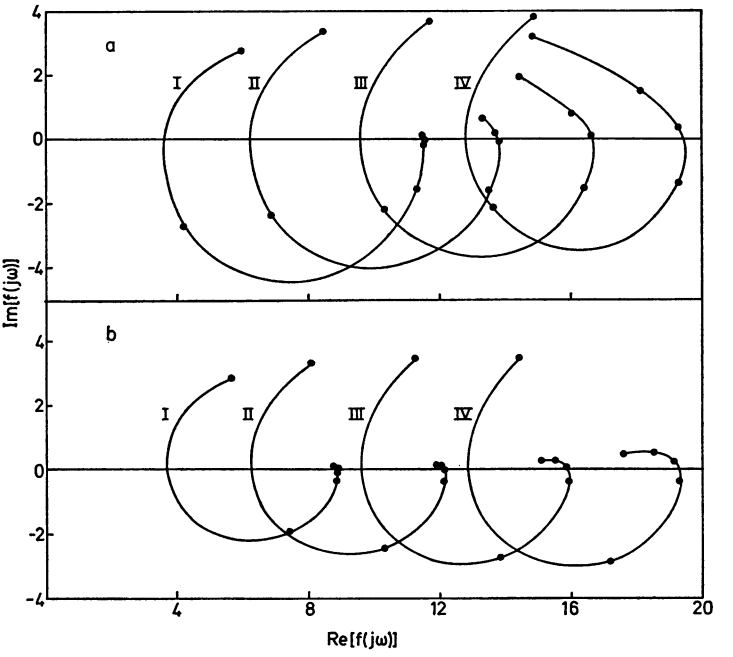

FIGURE 6 Nyquist plots comparing the effect on frequency-response shape of variation of the A-filament stiffness in equation 22, for both A-filament-strain activation (*a*) and A-I displacement activation (*b*), as discussed in the text. Units for the real and imaginary axes are (dynes per A-filament per micron extension of the simulated 1.2-micron half-sarcomere) $\times 10^4$. The points denote the frequency loci of the complex stiffness at each decade of the 0.001-to-100 cps range, frequency increasing clockwise. (*a*) The product $(Q \cdot F) = 0.05$ dyne/micron-sec, $R = 0.0$; (*b*) The product $(R \cdot F) = 0.25$ dyne/micron^2-sec, $Q = 0.0$, $p_d = 30$ sec^{-1}; k values for both *a* and *b*, I–IV: 4, 7, 11, and 15 $\times 10^{-4}$ dynes, respectively. Other parameters are as in Table I.

therefore increase with reduced k—in contrast to those for R activation in Fig. 6 *b*. These effects demonstrate that the expected interactions between the structure of Fig. 3 and the rules for the generation of bridge force do occur.

Comparison of Predicted Average Cycling Rate and Experimentally Determined ATPase Activity

It has been shown that the dynamics of the two-state cycle, with detachment rate constant, p_d, determining the primary delay between length and tension, can account for the mechanical experiments of Fig. 5. An independent test is to compare the predicted average cycling rate of the cross bridges, using the parameters fixed in obtaining the agreement of Fig. 5, with experimental measurements of rate of hydrolysis of ATP.

In the model of Fig. 2, the average attach-detach cycling rate at low degrees of activation (i.e., under conditions in which the number of attached bridges is small)

is given approximately by the product of the average value of the attachment rate constant, p_a, and the number of bridges available. Under conditions of strain activation, p_a was taken as directly proportional to the strain in the A filament, the constant of proportionality (Q) being known as the strain-activation coefficient.

The comparison of prediction and mechanical data in Fig. 5 has been shown above, under the assumptions underlying equation 22, to specify uniquely a value of the product $(Q \cdot F)$ associated with each level of Ca^{2+} concentration employed in the experiments of Fig. 5 *a*. In Fig. 5 *b* the 1-cps stiffness increment corresponding to that for muscle fibers activated at a pCa of 7.48 was given by $(Q \cdot F) = 0.037$ dyne/micron-sec-unit A-filament strain. A value of Q appropriate to the prediction of cycling rate in the model can therefore be derived from this product if an independent estimate for the value of F is obtained.

The bridge force per unit length of A filament (F) can be given a lower bound from counts of the number of A filaments and from the largest tensions known for the muscle. White (1967) has measured tensions of 35 dynes per fiber at 1% stretch in high Ca^{2+} concentrations. Since there are about 6×10^5 A filaments in a cross-section of a fiber (Chaplain and Tregear, 1966), and the tension is transferred to the I filaments over each 1-micron overlap region, F is at least 6×10^{-5} dyne/micron. From the above estimate of the product $(Q \cdot F)$, Q is therefore at most 6×10^2 sec^{-1} per unit A-filament strain.

The average value of p_a in the model is the product of Q and the average strain in the A filaments. At 1% sarcomere strain in the *passive* case, the elasticity of the C-filament region in Fig. 3 allows only about one quarter of the strain in the sarcomere to appear in the A filaments (White, 1967). Under the conditions of activation simulated, however, the average A-filament strain at low frequencies is closer to one-half of the total sarcomere strain. Thus the predicted dependence of the mean attachment rate constant, $\bar{p}_a$, on steady stretch (6×10^2 sec^{-1} per unit A-filament strain) corresponds to 3 sec^{-1} per % sarcomere strain. (This estimate is consistent with the assumptions since the corresponding average fraction of bridges attached, $\bar{n}$, at 1% stretch is $\bar{p}_a/(\bar{p}_a + p_d) \doteq 0.12$, in keeping with the low-Ca^{2+} requirement that $n \ll 1$. Conversely, the assumption that n is small in the range of stretches used to fit the low-Ca^{2+} data is consistent physically with the known maximum tensions produced by the muscle.) If there are 300 cross bridges per A filament, and the sarcomere length is 2.4 microns (Chaplain and Tregear, 1966), the corresponding cycling rate of cross bridges is 1.3×10^{14} bridge cycles/cm fiber-min-% stretch. If one molecule of ATP is hydrolyzed per cross-bridge cycle, the predicted value for ATPase activity, to be compared with experimental values, is 200 pmole/cm fiber-min-% stretch at pCa 7.48 and 22°C.

In the experiments of Rüegg and Tregear (1966, Fig. 5), Ca^{2+}-activated ATPase activity increments vs. steady stretch in *L. cordofanus* fibers at 18–23°C were approximately 25 pmole/cm fiber-min-% stretch at pCa 7.4, and as large as 300 pmole/cm fiber-min-% stretch at pCa 7.0. In more recent measurements on *L. cordofanus* done

at Ca^{2+} concentrations which bracket the pCa value of 7.48 taken for the above calculations, Chaplain (1967, Fig. 2) finds slopes of about 70 and 320 pmole/cm fiber-min-% stretch at pCa 7.6 and 7.3, respectively, at 23°C. The discrepancy between the prediction and the measurements of Rüegg and Tregear is in the most likely direction—the prediction is an overestimate based on the underestimate of realizable bridge force, while the experimental values probably tend to be low. The agreement with Chaplain's experiments is striking.

Nonlinear Properties of the Cycle

Since the specific assumptions made about cross-bridge activation have not led to discrepancy in comparisons with the small-signal mechanical and chemical data, it is of interest to compare their consequences with experimental data for larger length changes. Since the relation between p_a and n is nonlinear for the case in which $n(x, t)$ is not small, some of these effects are estimated here in the following way: in the small-signal case, the distributed viscoelastic effects for the particular passive structure used did not appreciably alter the qualitative dynamic predictions one would have made from the equations for a single cycle of cross-bridge activity, with active tension simply added to that of the passive muscle. We therefore feel justified in ignoring the distributed effects in a preliminary study of the nonlinear behavior of the cycle at slightly larger amplitudes of oscillation.

For step changes of p_a and p_d in equation 1, a general solution is

$$n(t) = n_0 + (n_\infty - n_0)\,(1 - e^{-(p_a + p_d)t}) \qquad (1b)$$

where

$$n_0 = \frac{p_{a_0}}{p_{a_0} + p_{d_0}}$$

$$n_\infty = \frac{p_a}{p_a + p_d}.$$

p_{a_0} and p_{d_0} denote values of the rate constants at $t < 0$, whereas p_a and p_d denote the constant values to which the rate constants are changed at $t = 0$. The steady-state fraction of bridges attached is therefore n_∞, and the steady cycling rate of bridges is given by

$$n_\infty \cdot p_d = (1 - n_\infty) \cdot p_a = \frac{p_a \cdot p_d}{p_a + p_d}$$

With $p_a \ll p_d$, as assumed in the low-Ca^{2+} small-signal analysis, the equilibrium value of n was given approximately by p_a/p_d. Although it was assumed for definiteness that the cycle was perturbed through small increases of p_a following small increases of strain, the alternative view that small increases of strain produced small

decreases of p_d would have produced identical small-signal dynamics—the average steady value of p_d still determining the rate limitation on stretch activation. In the nonlinear case, these alternatives are eminently distinguishable; we illustrate this distinction below by comparison with Tregear's (1967) data for large amplitudes of length oscillation.

Fig. 7 *a* shows some of the stretch-amplitude-dependent nonlinearities measured in Ca^{2+}-activated glycerinated water-bug flight muscle when stretch is modulated by 1–2% about a steady stretch of 2–3% over zero-tension length. A summary of these and other nonlinear effects is as follows (Tregear, 1967):

(*a*) The counterclockwise length-tension loops in Fig. 7 *a* (measured during performance of oscillatory work) change from the ellipses shown at small amplitude to the clamshell-shaped loops at higher amplitude. These are usually pointed at the bottom at the frequency of maximum work, but the vertical position of the smallest ellipse with respect to the largest is variable.

(*b*) Tension transients following large steps of length are asymmetrical; although not characterized by a simple exponential, the rise of tension is slower than the decay (Fig. 7 *a*).

(*c*) Average ATP-splitting rate increases with degree of steady stretch, saturating near 6% stretch as in Fig. 7 *a* (Rüegg and Tregear, 1966).

(*d*) Steady active tension (T) vs. steady stretch (L) rises nonlinearly (in the sense: $T \propto L^h$, with $h > 1$).

(*e*) An oscillation amplitude is increased about a given degree of stretch, the average ATPase rate during oscillation increases (Rüegg and Tregear, 1966).

(*f*) Although the frequency-dependent nonlinear effects have not yet been studied thoroughly, there are indications that the clamshells of Fig. 7 can at higher frequency collapse into figure-8's (Tregear, 1967); that is, the fundamental component of stretch-activated tension is apparently attenuated at a lower frequency than are the higher harmonics.

In order to compare the two-state-cycle hypothesis qualitatively with the above effects it is assumed that, in equation 1, cycling rate is commensurate with the rate of ATP hydrolysis and the fraction of attached bridges, n, is commensurate with tension. Various parameters, to be specified, will be assumed to be forced according to linear functions of length. Furthermore, only the active component of stiffness is estimated, so that the sharp leading edge of the experimental step response in Fig. 7 *a*, for example, is not simulated.

First, consider the effect of forcing p_a such that p_a is directly proportional to length, and keeping p_d constant. Since the steady value of n for the cycle is $p_a/(p_a + p_d)$ it is clear that the resulting steady-state tension-length curve shows monotonically decreasing stiffness with increasing length, whereas, experimentally, the stiffness is monotonically increasing. The average cycling rate, $p_a p_d/(p_a + p_d)$, as a function of stretch, on the other hand is in qualitative agreement with experiment, as shown in Fig. 7 *b*. However, analog-computer solutions for the dynamic variation

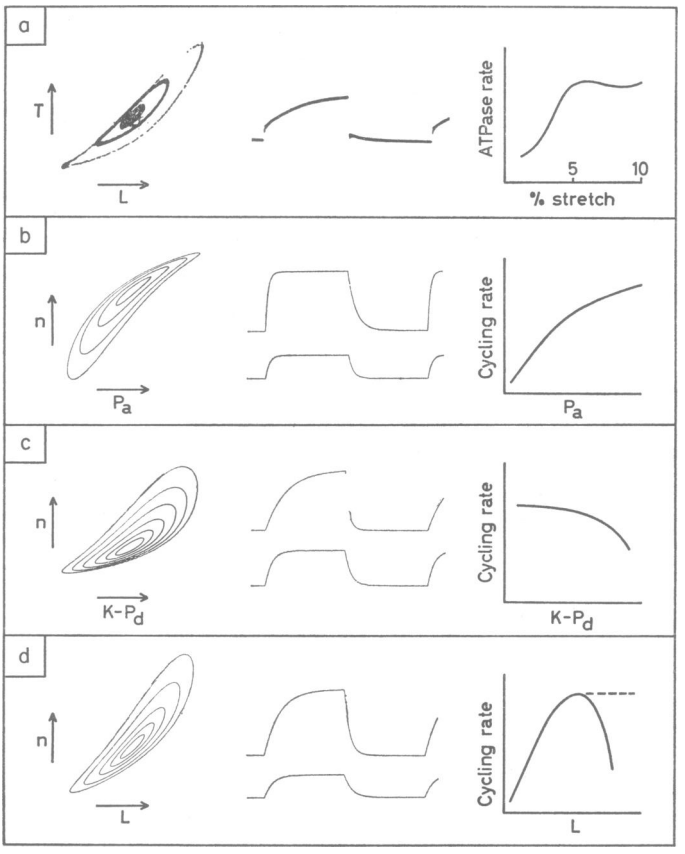

FIGURE 7 Qualitative large-signal nonlinear behavior of glycerinated fibrillar muscle (*a*) and of the attached-detached cycle (*b–d*). (*a*) Left: Tension-length loops as length-oscillation amplitude is increased beyond the linear range; largest loop represents 15 dyne/fiber peak-to-peak tension under 2.7% peak-to-peak length variation on 2% steady stretch (White, unpublished). Center: Asymmetrical tension response (40 mg/fiber peak-to-peak) to 1-cps square waves of length change (2.2% peak-to-peak) (Tregear, 1967). Right: form of average ATP-splitting rate vs. steady stretch of the muscle (from Rüegg and Tregear 1966). (*b–d*) Results of simulating the above three experiments with equation 1 on the analogue computer as described in the text. (*b*) Modulation of p_a by length such that p_a = constant × length. $\bar{p}_a = p_d$ (the bar denotes time averaging). Modulation ranges of p_a : 20–90% (loops); 20 and 100% (steps); 100% (cycling rate). (*c*) Modulation of p_d by length such that $p_d \propto k -$ length. The abscissa is therefore of the form length $\propto k - p_d$ where the constant k is such that $\bar{p}_d = 8p_a$. Modulation ranges of p_d : 15–80% (loops); 15–80% (steps); 100% (cycling rate). (*d*) Modulation of both p_a and p_d by length as described in the text. $\bar{p}_d = 3\bar{p}$. Modulation ranges of length: 15–75% (loops); 20 and 90% (steps); 100% (cycling rate). In *b*, *c*, and *d*: *n* is in arbitrary units; the upper (large-signal) step-response scale is one-fifth that of the lower. The nonlinear behavior is determined by the ratio $\bar{p}_a/\bar{p}_d$, whereas the frequency of maximum phase lag is determined by $\bar{p}_a + \bar{p}_d$. Forcing frequencies for the loops and steps are therefore left in arbitrary machine-time units, but are the same for all loops or steps in each diagram.

of n as p_a is forced sinusoidally or by steps in the region of the nonlinear response show that both the clamshell effect and the asymmetrical response to steps of length are opposite in sense to the coresponding experimental effects.

Consider now the effect of forcing p_d such that p_d decreases linearly with increase in length. It has already been stated that this alternative gives a small-signal response identical to that obtained by forcing p_a as above. Since p_d must have a value of about $10 \cdot p_a$ at 1% stretch, forcing p_d in this manner gives the correct form for the active tension-length curve. It is shown in Fig. 7 *c* that sinusoidal and step forcing of p_d produce responses which simulate qualitatively the experimental dynamic nonlinearities, apart from the initial transient changes noted previously. However, as also illustrated in Fig. 7 *c*, as p_d is reduced over the appropriate range, the average cycling rate is monotonically decreasing—opposite to the behavior of the experimental ATPase rate vs. stretch.

Before the nonlinear behavior of the two-state cycle is judged insufficient on the basis of the above paradoxes, it should be noted that appropriate simultaneous forcing of both p_a and p_d in opposite directions can remove much of this disagreement. In Fig. 7 *d*, analog-computer solutions are shown in which p_a and p_d are forced by length, L, according to the following relationships:

$$p_a(t) = C_1 \cdot L(t)$$

$$p_d(t) = C_2 - C_3 \cdot L(t)$$

where the C's are constants. The mechanical tension-length nonlinearities associated with p_d are then partially retained, and at the same time the cycling rate rises at low degrees of stretch because of the variation of p_a.

This type of control of the rate constants is in the direction expected if p_a were perturbed by a correlate of stretch, and if a product of the attachment process (e.g., in the formulation of Fig. 1, ADP) had the effect of stabilizing the attachment of bridges to the actin (Chaplain, Abbott, and White, 1965; Abbott[1]; Pringle, 1967), thereby effectively reducing p_d. If the availability of such a product were directly proportional to the instantaneous cycling rate, $p_a(t)\ (1 - n(t))$, then p_d might more properly be determined by a relationship of the form

$$p_d(t) = \text{constant} - p_a(t)\ (1 - n(t)).$$

The reduction of p_d is then self-limiting (as n approches unity) and the cycling rate saturates at high stretch as shown by the dotted line in Fig. 7 *d*. Under these conditions, however, the type of nonlinear response to step and sinusoidal changes of length shown in Fig. 7 *d* occurs only in the lower half of the region of average stretch simulated.

Finally, it can be shown that neither of the experimental effects (*e*) and (*f*), above, can be simulated by means of the assumptions used here. Time averages of the

instantaneous cycling rate during large-signal forcing tend to decrease slightly with increased amplitude (cf. *e*). Moreover, figure-8's do not occur at high forcing frequencies. Since higher harmonics in the model are generated within the cycle, they are attenuated more rapidly, as forcing frequency is increased, than is the fundamental (cf. *f*).

Therefore, even though certain of the measurable nonlinearities arise quite naturally in the two-state cycle, it is concluded that one cannot account for the entire nonlinear behavior of the muscle by means of a simple forcing of this cycle in the manner treated above. Unfortunately, the likely presence of unknown nonlinearities means that this failure does not restrict the original small-signal formulation. Rather, the discrepancies noted suggest specific ways in which the outline originally presented in Fig. 2 might be modified. First, in order to account for the static tension-length nonlinearity (property (*d*) above), either a nonlinearity external to the cycle (e.g. p_a a nonlinear function of strain), or considerable dependence upon control of p_d by length, as in the examples above, is indicated. Also of concern here are sources of nonlinearity attributable to the passive muscle, or to differences in the states of the various myofibrils in a fiber as mounted in the apparatus. Second, the failure of the cycle to exhibit extra average APTase activity during large-signal oscillation (property (*e*) above) could be rectified in terms of a three-state descritpion of cross bridges in which oscillation recruits an increased population into the active attach-detach cycle. Pringle (1967, p. 49, property viii) has already discussed a related mechanism, in that his detached bridges may be in either of two states, depending on tension in the A filaments. Third, there is considerable information in the tendency of the large-signal length-tension loops to assume figure-8 shapes at high forcing frequencies, since the effect indicates a nonlinearity which is either external to the attach-detach cycle or strongly frequency dependent. Fourth, in considering length changes for which appreciable changes in the configurations of the cross bridges occur during attachment, one ought to estimate effects of the associated changes in shear force (A. F. Huxley, 1957). Preliminary calculations based on the probability density function of bridge-attachment time show that these effects can produce asymmetric nonlinearity of the kind illustrated in Fig. 7 *a*.

DISCUSSION

The analysis presented in this paper makes a strong case for further consideration of the dynamic behavior of cross-bridge detachment as a rate-limiting factor in stretch activation. Each of the quantitative tests to which the model was subjected—the dynamic mechanical analysis and the comparison with ATPase activity—was a priori capable of producing severe arguments against it; yet both led to rather remarkable agreement. Before further implications of this view of the muscle are outlined, two earlier and distinctly different suggestions for the origin of the delay in tension following stretch will be discussed briefly.

R. H. Abbott (1965)[4] pointed out that the ADP-diffusion rate constant for diffusion out of the fibers agrees approximately with the limiting rate constant for delayed tension in small-signal experiments (20–40 sec^{-1}); therefore, if tension were by any means proportional to available ADP in the fiber, exponential delays at commensurate frequencies might be expected since ADP concentration would not change at rates much beyond its loss rate. Abbott predicted from such considerations that addition of ADP should increase tension even when ATP is in excess and that ATPase activity should increase with stretch—effects which have subsequently been observed (Chaplain, Abbott, and White, 1965; Rüegg and Tregear, 1966). It should, therefore, be made clear that the hypothesis of this paper—leading to assignment of the delay in tension to p_d—is consistent with both (*a*) the view that ADP diffusion has a rate constant similar to that for delayed tension (since change in ADP availability is not a rate-limiting event in the formulation of this paper), and (*b*) the observation that extra ADP can increase tension (if it is assumed that the average value of p_d is reduced somewhat by certain changes of chemical conditions, as in the example of the previous section). Although Abbott's suggestion has not been formulated with respect to the dynamics of actin-myosin shear force, such distinct alternatives may be separable by experiment—particularly by prediction and measurement of transient changes in cyclic work as state of stretch is changed.

Another distinct hypothesis for the delay in tension in fibrillar muscle has been formulated by Pringle (1967). The suggestion is that the delay may arise because it takes time for attached bridges to change their configurations and produce strain in the filament structure. To the extent that such a velocity limitation on angular motion of an attached bridge can be represented as an effective interfilament viscosity, the formulation in Fig. 3 allows one to argue that this suggestion is inadequate, at least for the small-signal case. In Fig. 3, consider for the moment that changes in $f(x, t)$ are not rate-limited by p_d as in the present example; the interfilament viscosity H is then analogous to the delay-determining factor in the above proposal. For the values of the passive-muscle parameters used, however, increasing H tends at a given frequency to produce a greater phase *lead* of tension with respect to length—in the direction opposite to that of the desired delay. This effect of H is discernable in the explicit form of the region-2 rate constant derived in the Appendix; a reduced rate constant moves the curves of Figs. 4 *b* and 5 to the left on the frequency axis. Pringle's consideration that delay can be involved in building up strain is of course in principle valid (it is analogous to the delay associated with a series elastic element and parallel viscosity as invoked by Hill (1938) for the events following nerve-impulse activation in vertebrate muscle). It is suggested here, however, that under low-$[Ca^{2+}]$ strain activation of the relatively rigid fibrillar muscle, the passive interfilament viscosity produces primarily a phase lead of tension with respect to length. It should be clear that this observation relates only to the basis of delay-production,

[4] Abbott, R. H. 1965. Personal communication.

and that Pringle's (1967) general model summarizing the geometrical and chemical parameters of the cross-bridge cycle is not in question.

Armstrong, A. F. Huxley, and Julian (1966) have shown that frog semitendinosus muscle in tetanus will respond with delayed tension changes to sufficiently small changes of length. The behavior differs from that measured in insect flight muscle, however, in that the delayed tension decays rapidly to nearly the pre-step value. Any view of the mechanism of stretch activation in insect muscle is of course an hypothesis for this phenomenon in frog muscle; the structure of Fig. 3 is further consistent with the transient nature of the delayed tension: White's (1967) comparison of vertebrate- and insect-muscle A-I band ratios with passive stiffness values suggest that passive vertebrate muscle can be represented with parameters similar to those in Table I, but with the C-filament length increased several fold. The resultant highly compliant C-region permits very little low-frequency or static strain of the A filaments. Stretch activation is therefore induced only by viscous effects and cross-bridge forces during rapid changes of length, and is not maintained. The argument is of course similar if there is no structure corresponding to the C filament in vertebrate muscle.

The calculation in this paper of the effects of the distributed viscoelastic lattice, including cross-bridge "interaction," on the transformation of local cross-bridge dynamics to length-tension dynamics of the sarcomere has application beyond the use of it above. The method is readily extended to new rules for actin-myosin interaction and, with numerical integration of the differential equations, to a more general nonlinear description of the sarcomere. One by-product of the calculation is already clear: Machin and Pringle (1960) and Abbott[1] have subtracted vectorially the passive complex stiffness of the muscle from the active complex stiffness, and used the resulting "difference plot" to suggest dynamic properties of the activation process. If the cross bridges interact this procedure of course gives a distorted estimate of the local active process. Our calculations serve as a control on this distortion—they show that, for the cases treated, one gets *qualitatively* similar dynamics with or without consideration of the full structure of Fig. 3. However, the distributed effects (as demonstrated in Fig. 6) can be sufficiently powerful to require caution in a quantitative interpretation of difference-plot shape to determine local active events.

Finally, the present formulation suggests a novel line of experiment. Since the suggestion that cross-bridge detachment rate p_d provides a critical rate limitation for stretch activation in glycerinated water-bug flight muscle has held up under several tests, consider for the moment the view that this rate constant is also important in the flight apparatus of all insects having fibrillar muscle. In terms of natural frequency of wingbeat, these range from a few per second to nearly 1000 per second in certain midges (Sotavalta, 1953). Although mechanical factors are obviously involved, the implication of p_d suggests that accompanying biochemical adaptations may be correlated with efficient flight at such widely different wingstroke rates. For example, a comparative study of actin-myosin dissociation rate in vitro, to the extent

that this measure reflects cross-bridge detachment rate, would on this view produce a positive correlation between dissociation rate and natural wingbeat frequency.

SUMMARY

1. It is often assumed in the sliding-filament theory of muscular contraction that tension is generated by means of the cross bridges exerting a shear force between the thick (A) and thin (I) filaments. A theoretical analysis is presented of a two-state cycle of cross-bridge activity, similar to that considered by A. F. Huxley (1957), in which the bridges are either attached to, or detached from, the I filaments. It is shown that if a mechanical correlate of stretch perturbs the rate constants in this cycle, then exponentially delayed tension changes follow imposed changes of length; this suggests a possible explanation of the length-tension dynamics of insect fibrillar muscle at low Ca^{2+} concentration.

2. In order to test this hypothesis quantitatively the length-tension dynamics are calculated for a viscoelastic sarcomere in which local cross-bridge force generation obeys appropriate rules. For the small-signal case, simultaneous third-order partial-differential equations are used to represent plausible viscoelastic properties of the actin and myosin filaments, and their interaction by both viscous and cross-bridge forces. Bridge force is represented as a continuum of tension transfer between the A and I filaments, and is allowed to vary both with time and with position along the sarcomere. The magnitude of the bridge force at any point along the sarcomere is determined by the local fraction of bridges attached, which is in turn influenced by mechanical correlates of stretch. The representation of the sarcomere includes the region in which the A and I filaments overlap and the regions in which there is no overlap.

3. Comparison of prediction with small-signal frequency-response data, for the hypothesis that local A-filament strain perturbs either the attachment or the detachment rate in the above cycle, yields approximate agreement if (*a*) the average (unperturbed) detachment rate constant and (*b*) the strain-activation coefficient are chosen appropriately. The detachment rate constant, in this formulation, determines the exponential delay between length and tension.

4. The above restriction of detachment rate and activation coefficient—together with an independent estimate of realizable absolute cross-bridge force—specifies the average cycling rate of cross bridges in the hypothetical two-state cycle. Therefore, an independent test is to compare cycling rate in the model with experimental ATP hydrolysis rates. Again, the prediction is sufficiently close to the corresponding experimental values that the hypothesis is not restricted.

5. To emphasize that the above agreement does not specify the particular mechanical correlate of stretch chosen to perturb the cycle, an alternative postulate—that local A-I filament displacement, rather than A-filament strain, perturbs the cross-bridge attachment rate—is treated. Although these alternatives produce charac-

teristically distinct length-tension dynamics, both account approximately for available data.

6. Although certain of the large-signal nonlinear properties of insect fibrillar muscle arise naturally from estimates of the nonlinear behavior of the two-state cycle, complications accompany attempts to explain either the extra ATPase activity measurable at large amplitudes of oscillation or the frequency-dependent nonlinearity of the muscle.

7. None of the above tests excludes the starting suggestion that the cross-bridge detachment process is rate-limiting in stretch-activated tension changes for glycerinated water-bug flight muscle. Therefore the discussion is extended to show (*a*) that the notion compares favorably with two previous and distinctly different hypotheses for the origin of delayed tension following stretch in insect flight muscle and (*b*) that it suggests a new set of comparative measurements of actin-myosin dissociation rates in vitro.

APPENDIX

Derivation of the Transfer Function Relating Length and Tension for the Representation of a Half-Sarcomere Described in the Text

Partial differential equations for the idealized half-sarcomere, shown diagrammatically in Fig. 3, are derived subject to the following assumptions;

(*a*) The time-varying displacements of points on the filaments are small with respect to the dimensions of the system, so that local longitudinal displacement can be described as a function of absolute position as is done for example in describing a sound wave (see, e.g., Timoshenko, 1937). The experimental fibrillar-muscle data used for comparison in Fig. 5 were obtained with imposed sinusoidal length changes of 0.2% peak-to-peak.

(*b*) For these small displacements, A, I, and C filaments are characterizable as linear materials, i.e., in terms of distributed viscous forces proportional to relative velocity and by elastic forces proportional to strain.

(*c*) Interaction of adjacent filaments other than by cross bridges is limited to viscous shear force proportional to relative local velocity.

(*d*) All filaments of one type in a half-sarcomere are identical, so that the half-sarcomere can be represented as a sum of parallel force generators each described by the dynamics of one A filament surrounded by six I filaments. The latter are lumped into a single "I filament," making appropriate allowance for viscous geometry and sharing of strain (the net A-I ratio in water-bug muscle is 1 to 3).

(*e*) Forces associated with the acceleration of parts of the system are negligible with respect to viscoelastic forces at the accelerations involved (i.e., masses are taken as zero).

(*f*) Since the local cross-bridge shear force f in Fig. 3 represents an average over the nearly 10^6 A filaments in a cross-section of a fiber, and since there are about 150 cross bridges per half-sarcomere length of a single A filament (Chaplain and Tregear, 1966), it is assumed that the local force (influenced by local A-filament strain as in equation 2) can be represented as a continuum $f(x, t)$ over the region 2 in Fig. 3. All variables, as well as their first derivatives with respect to x and t, are therefore taken as continuous in each region—so that the sequential order of differentiation in x and t can be reversed where necessary.

(*g*) Since the ends of the I filaments are free, their description in terms of a single stiffness coefficient implies either that they can be compressed without buckling, or that they are held

in slight tension, at moderate stretch of the muscle, by a small remnant of bridge force even in the passive case (White, 1967).

From Fig. 3, with x and t the independent variables for space and time,

$y(x, t)$ = the (small) displacement in the x-direction of a point on the A or C filament (cm),
$z(x, t)$ = the (small) displacement in the x-direction of a point on the I filament (cm),
k = the stiffness times unit length of the A filament (dynes),
h = the stiffness times unit length of the I filament (dynes),
g = the stiffness times unit length of the C filament (dynes),
H = region-2 viscous interaction coefficient per unit length between A and I filaments (dynes-sec/cm²),
G = region-1 viscous interaction coefficient per unit length between C and I filaments (dyne-sec/cm²),
$f(x, t)$ = cross-bridge shear force per unit length (dyne/cm).

We assign

$T_A(x, t)$ = local tension in the A filament or C filament,
$T_I(x, t)$ = local tension in the I filament,
$T(t)$ = total tension in the two-filament system = $T_A(b, t) = T_A(m, t)$.

Physical considerations show that (the subscripts x and t denoting partial differentiation with respect to those variables)

$y_x(x, t)$ = the local A- or C-filament strain,
$z_x(x, t)$ = the local I-filament strain.

For $a < x < b$, shear force between A and I filaments is due both to bridge force and to viscous effects, and for $0 < x < a$, shear force between I and C filaments is due to viscous effects only.

It follows that for $0 < x < a$

$$T_A(x, t) = gy_x(x, t) \tag{3}$$

$$T_I(x, t) = hz_x(x, t) \tag{4}$$

$$T_A(x, t) + T_I(x, t) = T(t) \tag{5}$$

$$[T_A(x, t)]_x = -[T_I(x, t)]_x = G[y_t(x, t) - z_t(x, t)] \tag{6}$$

And for $a < x < b$,

$$T_A(x, t) = ky_x(x, t) \tag{7}$$

$$T_I(x, t) = hz_x(x, t) \tag{8}$$

$$T_A(x, t) + T_I(x, t) = T(t) \tag{9}$$

$$[T_A(x, t)]_x = -[T_I(x, t)]_x$$

$$= H[y_t(x, t) - z_t(x, t)] + f(x, t). \tag{10}$$

The procedure is to determine $T(t)$ for arbitrary forcing of the length $L(t)$ of the sarcomere. Since the effect of the spring between $x = b$ and $x = m$ can be incorporated, simply, once the length-tension transfer function for the region $0 < x < b$ has been determined, the boundary-

value problem is initially confined to the region $0 < x < b$. Boundary conditions (in the notation of Churchill, 1944) follow from physical consideration of Fig. 3:

$$\left.\begin{aligned} y(0, t) &= 0 \\ z(0, t) &= 0 \end{aligned}\right\} \text{(fixed ends at Z band)} \quad (11), (12)$$

$$\left.\begin{aligned} y(a - 0, t) &= y(a + 0, t) \\ z(a - 0, t) &= z(a + 0, t) \end{aligned}\right\} \text{(continuity of displacement at } x = a) \quad (13), (14)$$

$$T_A(a - 0, t) = T_A(a + 0, t) \text{ (continuity of tension at } x = a; \text{ implies via equations 5 and 9 that } T_I(a - 0, t) = T_I(a + 0, t)) \quad (15)$$

$$y(b, t) = L(t) \text{ (forcing function)} \quad (16)$$

$$T_A(b, t) = T(t) \text{ (implies via equation 9 that } T_I(b, t) = 0, \text{ in accord with the effectively free end of the I filament).} \quad (17)$$

The boundary-value problem of equations 3–17 can be solved in a number of forms. We have chosen to eliminate T_A, T_I, and z. We first take Laplace transforms of equations 3–17 and substitute for $f(x, s)$ from equation 2. In this all relevant initial conditions are arbitrarily set to zero since only the steady-state tension response of the linear system to sinusoidal forcing of $L(t)$ is required. Differentiation of the transforms of equations 6 and 10 with respect to x, and elimination of T_A, T_I, and z for each of the two regions, then lead to the third-order equations in $y(x, s)$:

$$y_{xxx}(x, s) - \alpha y_x(x, s) = -\gamma T(s), \quad 0 < x < a \quad (18)$$

$$y_{xxx}(x, s) - \eta y_{xx}(x, s) - \beta y_x(x, s) = -\delta T(s), \quad a < x < b \quad (19)$$

where

$$\alpha = Gs\left(\frac{1}{g} + \frac{1}{h}\right)$$

$$\beta = Hs\left(\frac{1}{k} + \frac{1}{h}\right)$$

$$\gamma = \frac{Gs}{gh}$$

$$\delta = \frac{Hs}{kh}$$

$$\eta = \frac{FQ}{k(s + p_d)}.$$

The boundary conditions (11–17) are similarly transformed and readily rearranged into seven independent constraints on $y(x, s)$ and its derivatives:

$$y(0, s) = 0$$

$$y_{xx}(0, s) = 0$$

$$y(a - 0, s) = y(a + 0, s)$$

$$\frac{Hg}{Gk} y_{xx}(a - 0, s) = y_{xx}(a + 0, s) - \eta y_x(a + 0, s)$$

$$\frac{g}{k} y_x(a - 0, s) = y_x(a + 0, s)$$

$$y(b, s) = L(s)$$

$$y_x(b, s) = \frac{T(s)}{k}$$

General solutions of equations 18 and 19 are (see, e.g., Murphy, 1960)

$$y(x, s) = C_1 + C_2 e^{\alpha^{1/2} x} + C_3 e^{-\alpha^{1/2} x} + \frac{\gamma}{\alpha} T(s)x, \qquad 0 < x < a \tag{20}$$

$$y(x, s) = C_5 + C_6 e^{\lambda_1 x} + C_7 e^{\lambda_2 x} + \frac{\delta}{\beta} T(s)x, \qquad a < x < b \tag{21}$$

where

$$2\lambda_1 = \eta + (\eta^2 + 4\beta)^{1/2}$$

$$2\lambda_2 = \eta - (\eta^2 + 4\beta)^{1/2}$$

and the C's are constants in x. The transform of the total tension $T(s)$, also a constant in x, appears in this formulation as a constant to be determined, along with the six constants of integration, by the seven boundary conditions. Substitution for $y(x, s)$ and its derivatives, from equations 20 and 21, in the seven boundary conditions yields seven equations in the seven unknowns $C_1(s)$ through $C_6(s)$ and $T(s)$. Solution of this system of equations determines $T(s)$ in terms of the forcing function $L(s)$—and therefore the desired length-tension transfer function. One could, of course, then substitute $T(s)$ and the other constants into equations 20 and 21 to determine the transfer function relating $L(s)$ and any of the displacements $y(x, s)$.

The length-tension transfer function $u(s)$ for the region $0 < x < b$, by the above procedure, is

$$u(s) = \frac{T(s)}{L(s)} = \frac{z_3 y_1 - z_2 y_2}{z_4(x_1 y_2 + x_2 y_1) - z_3(x_1 y_4 - x_4 y_1) - z_2(x_4 y_2 + x_2 y_4)}$$

where

$$x_0 = \frac{1}{k} + \frac{\delta}{\beta}\left(b\lambda_1 - 1\right)$$

$$y_0 = \frac{1}{k} + \frac{\delta}{\beta}\left(b\lambda_2 - 1\right)$$

$$x_1 = e^{\alpha^{1/2} a} - e^{-\alpha^{1/2} a}$$

$$y_1 = \frac{\alpha^{1/2}g}{k}\,(e^{\alpha^{1/2}a} + e^{-\alpha^{1/2}a})$$

$$y_2 = \frac{\lambda_1\lambda_2}{\lambda_2 - \lambda_1}\,(e^{\lambda_1(a-b)} - e^{\lambda_2(a-b)})$$

$$x_4 = \frac{y_0 e^{\lambda_1(a-b)} - x_0 e^{\lambda_2(a-b)}}{\lambda_2 - \lambda_1} - a\left(\frac{\delta}{\beta} - \frac{\gamma}{\alpha}\right)$$

$$y_4 = \frac{\lambda_1 y_0 e^{\lambda_1(a-b)} - \lambda_2 x_0 e^{\lambda_2(a-b)}}{\lambda_2 - \lambda_1} - \left(\frac{\delta}{\beta} - \frac{\gamma g}{\alpha k}\right)$$

$$z_2 = \frac{Hg\alpha}{Gk}\,(e^{\alpha^{1/2}a} - e^{-\alpha^{1/2}a})$$

$$z_3 = \frac{\lambda_1\lambda_2}{\lambda_2 - \lambda_1}\,[(\lambda_1 - \eta)e^{\lambda_1(a-b)} - (\lambda_2 - \eta)e^{\lambda_2(a-b)}]$$

$$z_4 = \frac{y_0\lambda_1(\lambda_1 - \eta)e^{\lambda_1(a-b)} - x_0\lambda_2(\lambda_2 - \eta)e^{\lambda_2(a-b)}}{\lambda_2 - \lambda_1} + \eta\frac{\delta}{\beta}.$$

The length-tension transfer function $v(s)$ for the entire half-sarcomere of Fig. 3 is then obtained by observing that the region $b < x < m$ is mechanically in series with the region $0 < x < b$:

$$v(s) = \frac{1}{\dfrac{1}{u(s)} + \dfrac{m - b}{k}}. \tag{22}$$

The procedural complications of obtaining the expression for equation 22 and of programming it for digital computation suggest caution. As a check we have worked independently from Fig. 3, programmed the complex arithmetic in different languages for different computers, and got identical frequency-response curves for both the passive and active cases.

Characteristic Rate Constants of Regions 1 and 2

Characteristic rate constants for regions 1 and 2 can be defined for the passive muscle from the arguments of the exponential functions in the transfer function. For the passive muscle $Q = 0$, and the arguments are respectively $(\alpha^{1/2}a)$ and $(\beta^{1/2}(b - a))$, giving $[a^2G(1/g + 1/h)]^{-1}$ as the rate constant for region 1, and $[(b - a)^2H(1/k + 1/h)]^{-1}$ for that of region 2. Both have the units (sec^{-1}).

Stiffness Under Static Conditions

The low-frequency stiffness of the region $0 < x < b$ in terms of the activation coefficient Q, obtained by letting $s \to 0$ in $u(s)$ (here we have derived analytically only the static case, but checked digitally that the low-frequency limit of $u(s)$ agrees), is

$$\frac{T}{L} = \left[\frac{P_d}{QF} + \left(\frac{a}{g} - \frac{P_d}{QF}\right)e^{\frac{QF}{kp_d}(a-b)}\right]^{-1} \tag{23}$$

This limit is properly independent of h (the I-filament elasticity), since bridge force in this example is determined solely by A-filament strain. As $Q \rightarrow 0$ this expression tends to

$$\frac{T}{L} = \left[\frac{b-a}{k} + \frac{a}{g}\right]^{-1}$$

which is by inspection the static stiffness of regions 1 and 2 in Fig. 3 when $f = 0$. This result is a further check of equation 22.

We thank Professor J.W.S. Pringle, F.R.S., for extensive assistance and advice, and R.H. Abbott, R.T. Tregear, and Professor A.F. Huxley, F.R.S., for important suggestions and discussions. We are especially indebeted to R.H. Abbott both for allowing us to compare our predictions with his data in Fig. 5, and for his advice on digital-computer application.

Computer facilities were generously provided by the Oxford Computing Laboratory (KDF-9), Dr A.C.T. North of the Molecular Biophysics Laboratory (Elliott 803A), and Dr D.C. Witt of the Oxford Engineering Department (EMI Analog Computer).

We gratefully acknowledge financial support in the form of a U.S. National Science Foundation Postdoctal Fellowship (John Thorson).

Received for publication 16 September 1968 and in revised form 11 November 1968.

REFERENCES

ABBOTT, R. H., and R. A. CHAPLAIN. 1966. *J. Cell Sci.* **1**:311.
ARMSTRONG, C. F., A. F. HUXLEY, and F. J. JULIAN. 1966. *J. Physiol. (London).* **186**:26P.
ASHHURST, D. 1967. *J. Mol. Biol.* **27**:385.
AUBER, J., and R. COUTEAUX. 1963. *J. Microscopie.* **2**:309.
BOETTIGER, E. G. 1957. *In* Recent Advances in Invertebrate Physiology. B. T. Scheer, editor. University of Oregon Publications, Eugene, Ore. 117.
VOM BROCKE, H. H. 1966. *Pfluegers Arch. Gesamte Physiol. Menschen Tiere.* **290**:70.
BROWN, B. M. 1961. The Mathematical Theory of Linear Systems. John Wiley and Sons, New York.
CHAPLAIN, R. A. 1967. *Biochim. Biophys. Acta.* **131**:385.
CHAPLAIN, R. A., R. H. ABBOTT, and D. C. S. WHITE. 1965. *Biochem. Biophys. Res. Commun.* **21**:89.
CHAPLAIN, R. A., and R. T. TREGEAR. 1966. *J. Mol. Biol.* **21**:275.
CHURCHILL, R. V. 1944. Modern Operational Mathematics in Engineering. McGraw Hill Book Company, New York.
DAVIES, R. E. 1963. *Nature.* **199**:1068.
HILL, A. V. 1938. *Proc. Roy. Soc. Ser. B Biol. Sci.* **126**:136.
HUXLEY, A. F. 1957. *Progr. Biophys. Biophys. Chem.* **7**:255.
HUXLEY, H. E. 1957. *J. Biophys. Biochem. Cytol.* **3**:631.
HUXLEY, H. E. 1963. *J. Mol. Biol.* **7**:281.
HUXLEY, H. E. 1964. *In* Muscle. W. M. Paul, E. E. Daniel, C. M. Kay, and G. Monckton, editors. Pergamon Press, New York. 3.
INGELS, N. P., JR., and N. THOMPSON. 1966. *Nature.* **211**:1032.
JEWELL, B. R., and J. C. RÜEGG. 1966. *Proc. Roy. Soc. Ser. B Biol. Sci.* **164**:428.
MACHIN, K. E., and J. W. S. PRINGLE. 1960. *Proc. Roy. Soc. Ser. B Biol. Sci.* **152**:311.
MARUYAMA, K., J. W. S. PRINGLE, and R. T. TREGEAR. 1968. *Proc. Roy. Soc. Ser. B Biol. Sci.* **169**:229.
MIHALYI, E., and A. G. SZENT-GYÖRGYI. 1953. *J. Biol. Chem.* **201**:211.
MURPHY, G. M. 1960. Ordinary Differential Equations and their Solutions. D. Van Nostrand, New York.

PERRY, S. V. 1965. *In* Muscle. W. M. Paul, E. E. Daniel, C. M. Kay, and G. Monckton editors. Pergamon Press, New York. 29.
PRINGLE, J. W. S. 1949. *J. Physiol.* (*London*). **108**:226.
PRINGLE, J. W. S. 1957. Insect Flight. Cambridge University Press, England.
PRINGLE, J. W. S., 1967. *Progr. Biophys. Mol. Biol.* **17**:1.
REEDY, M. K., K. C. HOLMES, and R. T. TREGEAR. 1965. *Nature.* **207**:1276.
RÜEGG, J. C., and R. T. TREGEAR. 1966. *Proc. Roy. Soc. Ser. B Biol. Sci.* **165**:497.
SOTAVALTA, O. 1953. *Biol. Bull.* **104**:439.
SPENCER, M., and C. R. WORTHINGTON. 1960. *Nature.* **187**:388.
TIMOSHENKO, S. 1937. Vibration Problems in Engineering. Constable & Co. Ltd., London, England.
TREGEAR, R. T. 1967. *Bioenergetics.* **2**:269.
WHITE, D. C. S. 1967. Ph.D. thesis. Oxford University, England.